The role of irradiance in controlling coralline algal calcification

Erik C. Krieger (erik.krieger@vuw.ac.nz)
Victoria University of Wellington
Wendy A. Nelson
University of Auckland
Johan Grand
Université de Paris, ITODYS, CNRS UMR 7086
Eric Le Ru
Victoria University of Wellington
Sarah J. Bury
National Institute of Water and Atmospheric Research
Amelie Cossais
Victoria University of Wellington
Simon K. Davy
Victoria University of Wellington
Christopher E. Cornwall
Victoria University of Wellington

Research Article

Keywords:

Posted Date: March 21st, 2022

DOI: https://doi.org/10.21203/rs.3.rs-923640/v1

Abstract

Coralline algae are an essential element of benthic ecosystems throughout the ocean's photic zone. Yet, the role of light in shaping the physiology of coralline algae from cold-water, low-light habitats is poorly understood. Here, we assess the calcification physiology of five cool-temperate coralline algae in response to different irradiances over three months. We show that in contrast to current models focused on warmer water species, previously observed enhancement of calcification rates by photosynthesis is largely limited to lower irradiances, and that the removal of CO_2 from the calcifying fluid (CF) is not the underlying mechanism of this enhancement. Instead, this likely occurs via two processes: 1) increased ion pumping rates to elevate the calcium carbonate saturation state in the CF; and 2) a higher daytime pH in the diffusion boundary layer that raises pH_{CF}. However, as irradiance increases, ion pumping becomes increasingly saturated limiting further enhancements. Our results also suggest the existence of two calcification strategies in coralline algae and indicate that magnesium incorporation is determined by the internal magnesium to calcium ratio $[Mg]_{CF}/[Ca]_{CF}$. This study adds to our mechanistic understanding of calcification in coralline and fills in much needed knowledge about the role of light in controlling their physiology.

Introduction

Coralline algae are a diverse, cosmopolitan group of calcifying macroalgae (Rhodophyta) that are amongst the most crucial ecosystem engineers and foundation taxa in the ocean's photic zone[1]. The reef systems and rhodolith beds that are created, supported, and maintained by coralline algae provide habitat and nursery ground for countless other algal, invertebrate and fish species[2–6]. Chemical cues produced by coralline algae are essential for the settlement and morphogenesis of numerous marine invertebrate larvae (e.g. coral, abalone, sea urchins)[7–10]. As primary producers and calcifiers, coralline algae not only form the base of many marine ecosystems, but also play a crucial role in local and global nutrient cycles and the long- and short-term storage of carbon[11–13]. However, the ability of coralline algae to fulfil their fundamental ecological roles is threatened by global change, particularly ocean acidification (OA) that reduces their calcification and inhibits recruitment[14–18]. The impacts of OA have been intensively researched and there is an improving understanding of how seawater potential of hydrogen (pH) and carbonate chemistry drive coralline algal calcification[18–20]. Such a comprehensive mechanistic understanding, however, is severely lacking for other environmental parameters, including key factors such as light. This is surprising, given the large suspected and reported influence of light on photo-physiology and calcification rates. Furthermore, light not only moderates other global change drivers such as OA, but its quality and quantity have decreased substantially due to anthropogenic activities in many locations[21–26]. This is an environmental issue likely to become more widespread and intense in many coastal areas, especially near urban centres[27,28]. Understanding the role of light in driving coralline algal calcification is thus of paramount importance if we wish to predict changes in distribution and function of these important foundation species.

It is widely recognised that increased light (and hence photosynthetic rates) drives increased calcification in many photoautotrophic calcifiers. This stimulating effect of light on calcification in coralline algae was identified in the early 1960's when it was discovered that calcification is much higher during the day than at night[29]. Many subsequent studies have confirmed this, and it is now well established that the calcification of coralline algae is light-enhanced and thus usually correlates well with irradiance and photosynthetic rate[30,31]. At night, coralline algae tend to dissolve due to the release of respiratory carbon dioxide (CO_2) which decreases pH at the surface of the thallus within the diffusion boundary layer[31–33]. The daytime increase in pH on the alga's surface, on the other hand, is the result of the removal of CO_2 (and/or bicarbonate (HCO_3^-) + hydrogen ions (H^+)) during photosynthesis[32,33]. This is thought to be the main driver of light enhanced calcification, as it creates favourable conditions for calcification by elevating the saturation state (Ω) and/or carbonate ion concentration ($[CO_3^{-2}]$) at the surface of the alga, with inference that perhaps this also occurs at the site of calcification[31,34,35]. However, for better studied taxa such as coccolithophores and corals, we know that light-enhanced calcification could also be the result of other processes. For these organisms, calcification is likely enhanced in higher irradiances by elevated pH, dissolved inorganic carbon and Ω at the site of calcification, *via* pumping protons (H^+) out and HCO_3^- and calcium ions (Ca^{+2}) into the calcifying fluid (CF)[20,36–39]. In this scenario, increasing photosynthesis would supply increased energy to allow for light-enhanced calcification[39–41].

Here, we explore the calcification physiology and photo-physiology of five coralline algal morpho-types as they respond to increasing light levels. For shallow subtidal coralline algae, we thus hypothesise that: 1) increased light will increase both photosynthetic and calcification rate. We also surmise that there are two most likely reasons for this occurring: elevated pH of the CF (pH_{CF}) and/or increased Ca^{+2} pumping, as seen in corals[36]. We therefore also hypothesise that, 2) any increase in the calcification rate will be associated with increased Ω of the CF (Ω_{CF}). However, under rapid calcification, the depletion of the internal calcium pool has been observed in both corals and coralline algae, which might lead to the incorporation of additional magnesium into the skeleton. Thus, we also hypothesise that, 3) if under high growth, calcium demand outstrips supply, we will see an increase in the skeletal magnesium (Mg) content. If high light causes photoinhibition and/or damage, we hypothesise that, 4) this will be reflected in a decreased photosynthetic rate, Ω_{CF} and calcification.

To test these hypotheses, we combined standard physiological methods with Raman spectroscopy, to assess the effects of four irradiances (daily doses 0.6, 1.2, 1.8 and 2.3, mol photons·m^{-2}·d^{-1}) on the calcification rate, Mg content and FWHM (Full Width at Half peak Maximum; an approximation of Ω_{CF}) of five temperate coralline algal species/species complexes with differing morphologies. Also, we measured associated photo-physiology to assess whether extremes in light (too high or too low) could cause stress, which would be apparent by reduced pigment content and biologically relevant decreases in photosynthetic efficiency, measured by the "variable fluorescence (Fv) normalised to maximal fluorescence (Fm)" parameter (Fv/Fm).

Material And Methods

2.1 Sample collection and field sites

Coralline algae were collected 10 days prior to the experiment from two field sites located in Te Moana-o-Raukawa Cook Strait, Te Whanganui a Tara Wellington, Aotearoa New Zealand (Site A/Sharks Tooth 41° 34’ 88”S, 174° 79’ 05”E; Site B/Breaker Bay: 41° 34’ 06”E, 174° 82’ 56”S; also see Fig. 1) using self-contained underwater breathing apparatus (SCUBA). Since morphological identification of coralline algae is notoriously difficult, divers were instructed to collect five morphologically distinct groups that *a priori* we considered most likely to be species or species complexes. These included three groups of non-geniculate (“thick” = *Phymatolithopsis repanda* n = 37; “smooth” = *Pneophyllum* spp. n = 37; and “foliose” = *Lithophyllum carpophylli* n = 48), as well as two groups of geniculate corallines (“fine” = *Corallina* spp. n = 39; and “robust” = *Arthrocardia* spp. n = 38). Taxonomic consistency of collected material was examined in the laboratory before the start of the experiment using morpho-anatomical characteristics and after the experiment using molecular tools (for details see Sect. 2.2). For collection, geniculate corallines were chiselled from the rock with the attaching crust to avoid damaging them. Cobbles or rocks covered with thick or smooth crusts were collected directly from the seafloor. The foliose coralline, *Lithophyllum carpophylli* (Heydr.) Heydr., was collected by using garden scissors to cut pieces (~ 5 cm length) of *Carpophyllum maschalocarpum*, which were overgrown by this epiphytic foliose crust that encircles *Carpophyllum* stipes. All samples were placed in separate zip lock plastic bags filled with seawater that were then placed in black plastic bags to reduce light stress and prevent physical damage, before bringing them to the surface. After collection, organisms were transported to the laboratory facilities within 20 minutes in cooler bins filled with ice and cool packs to further minimise thermal and light stress. At the laboratory, organisms were kept under low light levels (2–8 µmol photons m^{-2} s^{-1}) for two days to allow for slow acclimation to laboratory conditions. Subsequently, organisms were carefully physically cleaned of epibionts and labelled according to the morpho-anatomic classification. Epoxy (Z-Spar A-788 Splash Zone) was used to form a base for geniculate coralline algae and to cover crusts of other species on cobbles/rhodoliths. Specimens were then distributed into the experimental tanks. Each tank contained one specimen of at least three, but up to five, different species. Slow acclimation to experimental conditions was achieved by the stepwise increase of irradiance over the course of ten days. The experiment ran from the 17/02/2019 to the 13/05/2019 (85 days).

2.2 Species identification

To verify the taxonomic consistency of the species groups recognised using morph-anatomical characters, four specimens of each species (~ 10% of total samples) were randomly selected for DNA-based identification. This was done for all species except for *Lithophyllum carpophylli*, where morphological identification is considered to be reliable due to its unique growth form and host specificity[42].

For identification, deoxyribonucleic acid (DNA) was extracted from silica-dried samples using the Qiagen DNeasy Blood and Tissue DNA Extraction Kit (Qiagen GmbH, Hilden, Germany) following the

manufacturer's instructions and the protocol established by Twist et al.[43], with the only exception that samples were ground in 200 µL AL buffer with micro pestles. For species identification, the *psb*A marker was amplified and sequenced. Amplification of the marker was achieved by using one of two primer mixes (*psb*AF1/*psb*AR1 or *psb*AF1/*psb*AR2)[44]. The amplification protocol followed Twist et al.[43] with the exception that each PCR reaction contained 3 µL of 5:95 diluted DNA extract. Quality and size of the polymerase chain reaction (PCR) product was checked by gel electrophoresis (1% agarose). Products were then purified using ExoSAP-IT (Affymetrix Inc., Santa Clara, USA) and subsequently sequenced by Macrogen (Seoul, Korea). All products were sequenced in both directions. Sequences were imported into Geneious Prime 2019.2.3 (Biomatters, Ltd., Auckland, New Zealand), trimmed and aligned to generate a consensus sequence. These were then blasted against the National Centre for Biotechnology Information (NCBI) GenBank using the "blastn" function (https://blast.ncbi.nlm.nih.gov/) to check species identity.

The results from the molecular identification enabled the creation of species groups, allowing for the correct and standardised interpretation of the results. The sequences obtained were compared to the findings of Twist et al.[43] and showed that none of the four groups was consistently identified to the species level using morpho-anatomic characteristics, reflecting the well-known difficulties of this approach[43,45]. (Species codes below follow Twist et al.[43] and are based on sequence data and herbarium voucher material.) Samples previously grouped under *Pneophyllum* spp. contained two Corallinales species (~ 75% *Pneophyllum* sp. F and ~ 25% *Corallinales* sp. E). Similarly, *Phymatolithopsis repanda* samples contained two species of Hapalidiales (*Phymatolithopsis repanda* (= *Hapalidiales* ZT ~ 75% and *Hapalidiales* sp. D ~ 25%). The robust geniculate grouped as *Arthrocardia* spp. was revealed to consist of *Corallina* sp. (~ 75%) and *Arthrocardia* sp. B (~ 25%). The same result was obtained for the fine geniculate *Corallina* spp. (*Corallina* sp. ~75% / *Arthrocardia* sp. B ~ 25%). The following five groups/species (Fig. 2) will thus be used in the remainder of the text: smooth crust -> *Pneophyllum* complex; thick crust -> *Phymatolithopsis* complex; *Corallina/Arthrocardia* "fine"; *Corallina/Arthrocardia* "robust" and *Lithophyllum carpophylli*.

2.3 Experimental treatments and design

The study was conducted at the Victoria University Coastal Ecology Lab located on Wellington's Cook Strait coastline. The experiment consisted of four different treatments each representing different light levels (noon irradiance of 20, 40, 60 and 80 µmol photons·m^{-2}·s^{-1}; daily doses 0.6, 1.2, 1.8, 2.3mol photons·m^{-2}·d^{-1}). Levels were chosen to cover irradiances observed below the canopy in the shallow subtidal region (Fig. 3). Each light level was replicated at the tank level twelve times for a total of 48 experimental tanks. Six experimental tanks (~ 4 L each; 17.5 cm W x 23 cm L x 12 cm H) were organised together in one 60 L water bath (56 cm W x 76 cm L x 18.5 cm H). Thus, a total of eight water baths were used to accommodate all the experimental tanks that would subsequently be treated appropriately during statistical analyses. Each water bath contained between one to two experimental tanks from each treatment (see Supplementary Fig. S1). The location and number of tanks *per* treatment within the water bath alternated sequentially between the eight water baths for equal distribution of the experimental

tanks over the whole setup. Water baths themselves were distributed over two shelf levels due to logistical constraints.

2.4 Experimental conditions

2.4.1 Light

Light was provided by 72 W light emitting diode (LED) panels (Zeus 70, Shenzhen Ledzeal Green Lighting Co., Ltd, Shenzhen, China) mounted over each water bath. The LEDs followed a natural diel cycle and were designed to mimic a natural coastal underwater light spectrum[46] (Fig.4). Light increased gradually in two steps (06:30–09:30 and 09:30–12:30) to reach maximum light levels over noon (12:30–16:30) and decreased again in two steps (16:30–18:30 and 18:30–20:30). Different light levels in the individual tanks were achieved by covering them with coated metal mesh and various types of shade cloth. Light levels were checked regularly using an underwater photosynthetically active radiation (PAR) meter (Apogee MQ-510, Apogee Instruments, Inc., North Logan, USA) and light loggers (HOBO MX2202, Onset Computer Corporation, Bourne, USA) (results see Supplementary Table S1).

2.4.2 Seawater supply

The seawater used for the experiment was pumped directly from the shore in front of the laboratory facilities, sand-filtered (mesh size 10 µm) and then fed into the setup. Seawater was first passed through aquarium chillers to decrease temperature variability. Chilled water was collected in two intermediated tanks (one *per* shelf level with ~ 60 L in each; 56 cm W x 76 cm L x 18.5 cm H) and pumped from there into the header tanks (~ 20 L in each; 30 cm W x 25 cm L x 38 cm H) using submersible pumps (Jeboa DC-650, 200 $L \cdot h^{-1}$). There were a total of eight header tanks, and one header tank supplied each of six experimental tanks with 150 mL seawater *per* minute. These were equally distributed over two neighbouring water baths (three *per* water bath). Header tanks contained one pump (Jeboa DC-650, 650 $L \cdot h^{-1}$) for strong water mixing.

2.4.3 Seawater Carbonate chemistry

Seawater pH, temperature and total alkalinity (A_T) were measured in each header tank and in randomly selected experimental tanks of each water bath at regular intervals to assess long- and short-term variability of these parameters (results see Supplementary Table S1). The pH was measured using a pH meter (HQ40D equipped with IntelliCal PHC101 probe, Hach Company, Loveland, USA) calibrated on the total scale using Tris/HCl buffers (following Dickson et al.[47]). A_T was calculated with a modified Gran function[47]. Regular titrations (AS-ALK2, Apollo SciTech, USA) of certified reference material (CRM, Batch 176 provided by A.G. Dickson lab) yielded A_T values within ± 6 µmol kg^{-1}. Seawater carbonate chemistry was calculated with the “seacarb” package running in R[48].

2.5 Physiological measurements

2.5.1 Mean-net calcification

Mean-net calcifciation rates were quantified using the buoyant weight technique[49]. The difference in weight at the start and end of the experiment was converted into dry weight of calcite and used to calculate net calcification. Net weight changes were transformed into calcification rates (mg $CaCO_3$ cm^{-2} d^{-1}) by normalising for time of the experiment (in days) and surface area (in cm^2, for details see Sect. 2.6). To ensure the correct calculation of calcification rate for geniculate corallines, the weight of the epoxy bases had to be subtracted. Therefore, bases were weighed after the experiment following the complete removal of the algae, and the obtained weight was subtracted from the individual sample weight from each timepoint. Due to an increase in mortality of the epiphytic *L. carpophylli* and the epilithic *Pneophyllum* complex in the second half of the experiment, calcification rates for these species are based on the weight change of healthy specimens from the first half of the experiment (17/02/2019-02/04/2019; 44 days).

2.5.2 Raman spectroscopy

Confocal Raman spectroscopy was used to determine sample minerology and approximate calcifying fluid Ω. Measurements were conducted with a Horiba Jobin-Yvon Labram HR Raman spectroscope (Horiba France SAS, Longjumeau, France) using a green 514 nm Ar-ion laser following DeCarlo et al.[50]. The measurement was carried out with an 1800 grooves per millimetre grating, a liquid-nitrogen-cooled CCD for detection, in the backscattering configuration with a long working distance objective with 50x magnification and a numerical aperture of 0.5. Wavenumber calibration was achieved through the repeated analysis of a silicon substrate. Bleached skeleton samples were placed on glass slides and analysed manually. A total of 20 individuals *per* species (five *per* treatment) were analysed. For each individual, 15 spectra (integration 5 x 4 s) were obtained (five spectra each from three different growth margins). Low quality or contaminated spectra were excluded from the analysis. The minerology of the sample was determined by the presence and shape of two peaks. The v1 peak (1,085–1,090 cm^{-1}) which is indicative for $CaCO_3$ and the shape of the v4 peak (700–720 cm^{-1}) which indicates presence of aragonite (double peak) or calcite (single peak)[51]. FWHM and position of the v1 peak was used to determine Mg content and to approximate calcifying fluid Ω[50]. Abiogenic calibrations of Perrin et al.[52] were used to estimate mol% Mg after correcting for the divergence of the Si wavenumber obtained in this study and reported by Perrin et al[52]. The calculated Mg content was also used to account for the effects of high Mg content on FWHM. Residual v1 FWHM was considered a proxy for calcifying fluid Ω of high-Mg calcite.

2.5.3 Inorganic carbon use

Organic tissue carbon isotope values (the ratio of ^{13}C to ^{12}C, defined as $\delta^{13}C$ in units of ‰) were measured at the end of the experiment from samples taken from five individuals from each of the species and treatments. Inorganic material was removed by placing dried specimens in 1 M HCL until bubbling of material had ceased indicating complete removal of inorganic carbon. Remaining organic tissue was

washed with MillQ water and then dried in an oven at 75°C for at least 48 hours. Dry samples were ground to a fine powder with an agate mortar and pestle. Stable isotope analyses were carried out on a DELTA V Plus continuous flow isotope ratio mass spectrometer linked to a Flash 2000 elemental analyser using a MAS 200 R autosampler (Thermo-Fisher Scientific, Bremen, Germany) at the National Institute of Water and Atmospheric Research (NIWA) Environmental and Ecological Stable Isotope Facility in Wellington, New Zealand. ISODAT (Thermo-Fischer Scientific) software calculated $\delta^{13}C$ values against a CO_2 reference gas, relative to the international standard Carrara Marble NSB-19 (National Institute of Standards and Technology (NIST), Gaithersberg, MD, USA), which in turn, was calibrated against the original Pee Dee Belemnite (PDB) limestone standard and was then corrected for ^{17}O. Stable isotope ratios were expressed as delta values (δ) in *per* mil units (‰), which represent the ratios of heavy to light isotopes within a sample (R_{sample}), relative to the ratio in an international standard ($R_{standard}$) as:

$\delta = \left(\left(\frac{R_{sample}}{R_{standard}} \right) - 1 \right) \times 1000$. All estimates of variance were calculated to 1 standard deviation (SD).

Carbon isotope data were corrected *via* a two-point normalisation process[53] using NIST 8573 (USGS40 L-glutamic acid; certified $\delta^{13}C$ = -26.39 ± 0.09‰) and NIST 8542 (IAEA-CH-6 Sucrose; certified $\delta^{13}C$ = -10.45 ± 0.07‰). At the start of each run, %C values were calculated relative to a laboratory reference standard of DL-Leucine (DL-2-Amino-4-methylpentanoic acid, $C_6H_{13}NO_2$, Lot 127H1084, Sigma-Aldrich, Australia) which was also run every ten samples to monitor analytical precision and drift. An additional international standard (USGS65 Glycine; certified $\delta^{13}C$ = -20.29 ± 0.04) was run daily to check isotopic accuracy. Repeat analysis of international standards produced $\delta^{13}C$ data accurate to within 0.15‰ with a precision of 0.15‰ for international standards and 0.25‰ for an internal squid laboratory standard.

2.5.4 Light and dark short term-incubations

Standard closed-chamber respirometry and the alkalinity anomaly technique were combined to measure photosynthetic, dark respiration, and light and dark calcification rates. For short-term incubations, five different individuals from each species from each treatment were randomly selected. For dark incubations, only specimens from 20 and 80 µmol photons m^{-2} s^{-1} treatments were selected due to logistical constraints and the lack of a detectable impact of light treatment on dark respiration rate. Specimens were placed in clear glass containers (500 ml) which were closed under water in the header tanks, carefully avoiding enclosure of air bubbles. Closed containers, also containing a stirrer bar that was separated from the organism, were then placed on a submersible stirring plate (2mag MIXdrive6, 2mag AG, Munich, Germany). This plate was placed in a water-filled tank located under an LED panel that allowed correct adjustment of light levels. Temperature control during incubations was achieved by using a chiller and a submersible heater, that were both connected to an aquarium controller. Incubations were conducted in the afternoon (between 12:30 and 16:30) during the second half of the experiment (02/04/2019-13/05/2019). Dark incubations were started early in the morning before the specimens were exposed to the day's light to keep the photo-physiology consistent with what was occurring at night. Incubation times were adjusted to organism size and/or light level, and ranged between 1 and 2 hours.

Water samples and measurement of dissolved oxygen (O_2) (HQ40D equipped with IntelliCal LDO101 probe oxymeter, Hach Company, Loveland, USA) in header tanks were taken at the starting point. Changes in AT and O_2 were normalised for surface area, as well as water volume and incubation time, to obtain metabolic rates. Net photosynthesis was obtained by subtracting average dark respiration rate (20 and 80 only) from gross rate. Calcification was calculated based on the established stoichiometric relation of two moles A_T being removed for each mole of $CaCO_3$ precipitated. Chambers only filled with seawater which were also placed on the stirrer plate during incubations served as a control. Mean changes of A_T (2 µmol kg^{-1}) and O_2 (-0.1 mg L^{-1}) in control chambers were deducted from modification of these parameters caused by the organisms, but these are within measurement error.

2.5.5 Photosynthetic efficiency

The Fv/Fm of each individual coralline alga was measured at the start and end of the experiment using a Pulse Amplitude Modulated (PAM) chlorophyll fluorometer (Diving PAM/R, Heinz Walz GmbH, Effeltrich, Germany). Settings were adjusted for each species to ensure reliable results (measuring light intensity = 8 for *L. carpophylli*, *Corallina/Arthrocardia* "fine" and *Phymatolithopsis* complex; 7 for *Corallina/Arthrocardia* "robust"; 9–10 for *Pneophyllum* complex, gain = 1, damping = 2, saturation light intensity = 1, saturation pulse width = 0.8). Individuals were dark-adapted prior to each measurement for at least 30 minutes. Thus, measurements were only taken after 21:00 and if Fo > 120.

2.5.6 Light curves

Effective photosynthetic capacities and light acclimation state were assessed using the PAM's rapid light curve (RLC) function. Relative electron transport rates (rETR) were obtained over noon from five individuals from each species from each treatment. Individuals were exposed for 20 seconds to nine increasing light steps ranging from 0 to 198 µmol photons m^{-2} s^{-1}. Non-linear models were then fitted to the data, based on least-square error calculations to determine maximum relative electron transport rate ($rETR_{max}$), light use efficiency (α or initial curve slope) and minimum saturation intensity (E_k) (after Walsby[54]).

2.5.7 Pigment content

Pigment content was determined from samples taken at the end of the experiment. Therefore, fresh tissue samples were taken from five individuals from each species from each treatment. Red pigments (phycocyanin and phycoerythrin) were extracted using phosphate buffer (after Sampath-Wiley & Neefus[55]). Chlorophyll *a* (Chl *a*) was extracted using ethanol (after Ritchie[56]). Pigment absorbance was measured with a spectrophotometer (Evolution 300, Thermo-Fisher Scientific, Loughborough, UK) and content was calculated after Sampath-Wiley & Neefus[55] for red, and Ritchie[56], for green pigments.

2.6 Determination of surface area

Surface area of crustose species (*Phymatolithopsis* complex, *Pneophyllum* complex and *L. carpophylli)* was determined using the aluminium foil method[57]. The surface area of geniculate coralline algae (*Corallina/Arthrocardia* "fine" and *Corallina/Arthrocardia* "robust") was determined by establishment of a relationship between dry weight and surface area. Therefore, small pieces were cut from the thalli of silica-dried specimens. These pieces were then used to cover a 0.25 cm^2 quadrat. The pieces required to cover the quadrat were then weighed. This weight was assumed to be the weight corresponding to 0.5 cm^2 surface area, as there was photosynthetic tissue on both sides of the cut pieces. Mean weight was then doubled to get the dry weight that would correspond to 1 cm^2. Surface area of the individual specimen was calculated by dividing the calculated dry weight of that specimen (see Sect. 2.4.1) with the mean weight of 1 cm^2. Care was taken to get material from different parts (old and new growth) of the thalli to ensure a reliable relationship.

2.7 Statistical analysis

The effect of light on all measured parameters was examined using linear mixed effect models (R package "lme4") whenever possible. Light was used as a fixed effect, and water bath and header tank as random effects. Random effects were not used for respiration and dark calcification due to over parametrisation. Polynomial and linear models were both fitted to the data except for $rETR_{max}$, α, and E_k where a purely linear correlation with light was assumed. Models were then selected based upon R^2 and AIC. The assumptions of normality and equality of variance were evaluated through graphical analyses of residuals using the R software package "sjPlot". Treatment effects were determined using one-way Analysis of Variance (ANOVA) with p-values calculated using "lmerTest". Proportions of the variation (R^2) explained by the full models were calculated using the package "MuMin". Values with considerable leverage on model output and data structure were removed solely if organism health (i.e. bleaching) or external factors could explain disparity from other values. Such external factors were problems during measurement and/or data recording. All statistical analyses were performed with R[48].

Results

3.1 Mean-net calcification

Mean-net calcification of *Corallina/Arthrocardia* "fine", *Lithophyllum carpophylli*, and *Pneophyllum* complex was significantly affected by light, while no response was detected for *Corallina/Arthrocardia* "robust" and *Phymatolithopsis* complex (Fig. 5A). Average calcification rates of *Corallina/Arthrocardia* "fine" were up to two times greater at intermediate light intensities (0.05–0.07 mg $CaCO_3$ cm^{-2} d^{-1}) than under maximal and minimal irradiances (0.02–0.03 mg $CaCO_3$ cm^{-2} d^{-1}). Similarly, average calcification of *L. carpophylli* was seven to twenty times higher under intermediate light levels (0.10–0.13 mg $CaCO_3$ cm^{-2} d^{-1}) when compared with the lowest and highest irradiances (< 0.01–0.01 mg $CaCO_3$ cm^{-2} d^{-1}). Calcification of *Pneophyllum* complex increased linearly with light, from 0.07 to 0.17 mg $CaCO_3$ cm^{-2} d^{-1}.

3.2 Geochemistry

FWHM (the proxy for calcium carbonate saturation state at the site of calcification (Ω_{CF})) was significantly affected by light in two of the five species (Fig. 5B). In *L. carpophylli*, FWHM increased linearly with light from 0.21 to 0.82, while in *Corallina/Arthrocardia* "fine" a parabolic response was observed. The saturation was lowest under intermediate light levels (0.27–0.32) and highest under minimal and maximal irradiances (0.40–0.45). Mg content (Fig. 5C) only changed with light in two of the five species. In *L. carpophylli*, Mg incorporation decreased with light, from 16.83 to 14.42% Mg. In *Pneophyllum* complex, Mg content was highest under 80, 60 and 20 µmol photons m^{-2} s^{-1} (16.26–16.38% Mg) and lowest under 40 µmol photons m^{-2} s^{-1} (15.37% Mg). Analysed samples contained solely high-Mg calcite and no other minerals.

3.3 Net photosynthetic and dark respiration rates

Net photosynthesis was significantly affected by light levels in three of the five species (Fig. 5D), where photosynthesis increased linearly with increasing light levels in *Corallina/Arthrocardia* "robust", *Corallina/Arthrocardia* "fine" and *Phymatolithopsis* complex. In *Corallina/Arthrocardia* "fine", net photosynthetic rate increased linearly with light from − 2.73 to 69.34 µg O_2 cm^{-2} h^{-1}, while respective rates for *Phymatolithopsis* complex increased from − 0.38 to 4.91 µg O_2 cm^{-2} h^{-1}. In *Corallina/Arthrocardia* "robust", photosynthetic rate also increased linearly from 2.79 to 29.66 µg O_2 cm^{-2} h^{-1}. Dark respiration rate (see Supplementary Fig. S2) was not affected by light in any of the species.

3.4 Carbon isotopes

The was a significant effect of light on organic $\delta^{13}C$ values (see Supplementary Fig. S3) for two of the five species. In *Phymatolithopsis* complex, organic $\delta^{13}C$ increased linearly with light from − 22.49‰ to -15.33‰. In *Pneophyllum* complex, values were highest under intermediate (-23.05 to -20.31‰) and lowest under maximal and minimal irradiances (-23.52 to -24.48‰).

3.5 Light and dark calcification

Short-term light calcification was significantly affected by light in two of the five species (see Supplementary Fig. S4). In *Pneophyllum* complex, light calcification increased linearly from − 1.26 to 9.53 µg $CaCO_3$ cm^{-2} h^{-1}. In *Corallina/Arthrocardia* "robust", calcification was highest at maximal and minimal irradiances (1.15–8.22 µg CaCO3 cm^{-2} h^{-1}) and lowest under intermediate light levels (-35.34 to -14.72 µg $CaCO_3$ cm^{-2} h^{-1}). Dark calcification (see Supplementary Fig. S4) was only affected by light in *Phymatolithopsis* complex, where calcification was higher under minimum irradiances (1.99 µg $CaCO_3$ cm^{-2} h^{-1}) than under maximum irradiances (-17.79 µg $CaCO_3$ cm^{-2} h^{-1}).

3.6 Rapid light curves

Maximum saturation intensity (E_k; see Supplementary Table S2 and Supplementary Fig. S5) and maximum relative electron transport ($rETR_{max}$; see Supplementary Table S2 and Supplementary Fig. S5) increased with light in all species (except $rETR_{max}$ in *L. carpophylli*). Light-use efficiency (initial slope of the curve or α; see Supplementary Table S2 and Supplementary Fig. S5) only changed in *Corallina/Arthrocardia* "fine" and decreased with increased irradiance.

3.7 Photosynthetic efficiency

Photosynthetic efficiency (F_v/F_m), measured at the start and the end of the experiment, remained above 0.52 across all species and treatments (see Supplementary Fig. S6).

3.8 Pigment content

Chl *a* content changed with irradiance in three of the five species (see Supplementary Fig. S7). In *Phymatolithopsis* complex, Chl *a* content was highest at the intermediate light levels (0.10–0.17 mg g^{-1}) and lowest under minimum and maximum irradiances (0.05–0.07 mg g^{-1}). In the two geniculate species, Chl *a* content increased linearly with irradiance. In *Corallina/Arthrocardia* "fine", Chl *a* content rose from 0.39 to 0.57 mg g^{-1}, while in *Corallina/Arthrocardia* "robust" the content of this pigment increased from 0.29 to 0.52 mg g^{-1}. Content of the red pigments, phycocyanin (see Supplementary Fig. S7) and phycoerythrin (see Supplementary Fig. S7), was not significantly affected by irradiance in any of the five species.

Discussion

Our results contradict our *a priori* hypothesis (1) that light-enhanced calcification of coralline algae is always driven directly by increasing photosynthetic rate. While increasing irradiance benefits calcification here, this is limited at higher light intensities. The physiological mechanism invoked previously for light-enhanced calcification in coralline algae is that CO_2 is increasingly removed from the site of calcification for photosynthesis[31]. This model necessitates that light intensity, and both photosynthetic and calcification rates are positively correlated which each other. This however is not supported by our results. While photosynthetic rates did increase with light in all species, calcification predominantly peaked under intermediate irradiances (in 3/5 species). Only in one species was calcification rate positively correlated with photosynthesis and irradiance, whilst calcification of the fifth species was unaffected by light. The predominance of parabolic or negligible responses of calcification to light is surprising and contradicts the findings of many earlier studies that report an increase in growth with light[29,35,58,59]. Yet, there are studies that, like here, report a suppression of calcification in low-light adapted species at high irradiances[60,61]. Thus, it seems logical that calcification responses to irradiance are species and location specific and dependent on light acclimation status since suppression of calcification does not occur in high-light (e.g., tropical) species[62]. Additionally, many past comparisons only assessed responses under two light regimes (e.g. high *versus* low)[35,60,61,63], which excludes the detection of more complex non-

linear responses, such as the parabolic or tipping point responses identified here. Using an approach with numerous light levels enabled us to determine that faster photosynthetic rate does not always equate to faster calcification. In fact, calcification of low-light, temperate coralline algae can even decline as photosynthesis increases.

Our findings also shed new light onto the relationship between growth and Ω_{CF} (FWHM) in coralline algae and imply the existence of two calcification modes that coincide with two different morphologies. It is considered that coralline algae control Ω_{CF} by pumping ions (Ca^{+2}, HCO_3^-)[19] into or (H^+)[18] out of the calcifying fluid (CF) and facilitate calcification by elevating Ω_{CF} (our initial *a priori* hypothesis 2). The same physiological mechanisms support calcification of other taxa, for example corals. However, contrary to this, we show that faster calcification coincides with low FHWM in the two geniculate corallines. Yet, faster growth also coincides with higher % Mg, similar to *a priori* hypothesis 3. Mg incorporation is predominantly controlled by the seawater Mg to Ca ratio (Mg_{SW}/Ca_{SW} ~5.2)[64], with higher ratios equating to greater Mg content. Since this ratio was likely similar in all tanks, only changes in the species' internal ion balance (Mg_{CF}/Ca_{CF}) can account for the observed increase in % Mg. Therefore, it is likely that in the geniculate corallines, rapid calcification outstripped the supply with Ca which increased Mg_{CF}/Ca_{CF} ratios and decreased FWHM values, leading to the observed correlations. This is supported by similar observations made in faster growing corals and juvenile coralline algae[65,66]. Yet, it also implies that deficiencies in Ca supply are not uncommon in marine calcifiers, a process that might impair the ability of some species to rapidly calcify (e.g., as juveniles). We speculate that coralline algae substitute Ca with Mg under conditions in which a deficient Ca supply might otherwise hinder fast skeletogenesis.

Ca supply exceeds the demand, or is perhaps even upregulated, to facilitate growth in the slower growing non-geniculates. This creates a positive correlation between FWHM values and calcification rates and decreases % Mg. While this seems to occur in *Phymatolithopsis* complex, it is less clear for *Pneophyllum* complex and *L. carpophylli*. In *L. carpophylli*, calcification rates followed a parabola while FWHM values increased linearly. The opposite was observed for *Pneophyllum* complex. A parabolic trend for FWHM values in *Pneophyllum* complex is assumed despite the high variability in one treatment, potentially the result of diagenesis[67] or the inclusion of different materials (e.g. conceptacles)[68]. The discrepancy between FWHM values and calcification rates in these two species could be attributed to a time difference between the collection of both data sets and the normalisation of calcification rate to surface area, which introduced further variation here (where surface area and FWHM were assessed at t2 and calcification was assessed at t1). Indeed, uncorrected calcification rates (total gains in mg $CaCO_3$ d^{-1}) at the end of the experiment better reflect the geochemistry and support the existence of two calcification modes in coralline algae.

Increasing irradiance likely affects the calcification of coralline algae through a complex mix of two mechanisms: 1) increasing the supply of energy for ion pumping; and 2) altering the pH in the diffusion boundary layer (DBL) (pH_{DBL}). As outlined above, light-enhanced calcification is not caused by the

removal of CO_2 from the CF. We know from past research that dissolved inorganic carbon (DIC) in the CF $[DIC]_{CF}$ is elevated rather than depleted in coralline algae[19]. Due to the rapid equilibrium of seawater carbonate chemistry, elevated $[DIC]_{CF}$ would be impossible under a scenario of constant removal of CO_2. Yet, the correlation between pH_{DBL} and pH in the CF (pH_{CF}) indicates that the removal of CO_2 from the DBL also elevates pH_{CF}[35]. Here, it seems that light levels are not driving FWHM values, yet any pH_{CF} signal is most likely overwritten by changes in Ca_{CF}. Therefore, it is very likely that the removal of CO_2 from the DBL (but not CF) for photosynthesis does contribute towards higher daytime-calcification rates in coralline algae. However, as day-time calcification and photosynthesis increase with irradiance, the release of respiratory CO_2 at night lowers pH_{DBL} and increases $CaCO_3$ dissolution. This increase in dissolution at some point equalises daytime $CaCO_3$ accretion (peak of the calcification curve) and then surpasses it (decline in mean net calcification). Indeed, mean respiration (in 4/5 species) and dissolution rate (in 3/5 species) were generally elevated at high irradiance. Yet, pH_{DBL} is not the sole controller of growth.

Ion pumping to control Ω_{CF} is also likely to be extremely important in determining calcification rate. This is perhaps most easily seen in the non-geniculate corallines, where it appears that Ca pumping increased with light to support faster calcification. However, in two species, Ca pumping plateaued and then declined again at the highest irradiances, which coincided with a decrease in calcification. Since dissolution affects mean net calcification but not % Mg or FHWM values, the drop in calcification can be, in part, attributed to a decrease in Ca pumping. The reason is unclear and warrants further examination. Yet, it is possible that supply of energy plays a role. At first, ion pumping increases with light due to the concomitant increase in available energy, then becomes saturated (peak of the calcification curve) and then declines again at the highest irradiance. At this light intensity, photoinhibition and/or damage perhaps starts to become stressful, and energy is diverted away from ion pumping to alleviate this, similar to our *a priori* hypothesis 4. Pigment content, Chl *a* fluorometry and O_2 evolution measurements do not indicate an increase in photoinhibition. However, changes in the use of DIC towards more CO_2 and less HCO_3^- occurred in some species at higher irradiances, indicating a diversion of energy from these processes that could underlie some form of physiological impairment that is not otherwise measurable.

Our study species were highly sensitive to small changes in irradiance indicating that any modification of the underwater light regime is likely to negatively impact the biology and ecology of these coralline algae. In many coastal systems, the quality and quantity of light is substantially reduced by anthropogenic activities[21–26]. Our results show that even a small reduction in irradiance decreases photosynthetic output and calcification performance of coralline algae. As a result, we should expect further decreases in coralline algal abundance if human activities continue to reduce coastal light levels. Reductions in coralline algal abundance are likely to have strong negative impacts on reliant species and ecosystems. For example, settlement success of numerous marine invertebrates depends on the presence of specific coralline algal species[10]. In addition, coralline algae augment survival of adult kelp[69] and facilitate kelp recruitment[69,70]. Yet, kelp recruitment can also be suppressed by coralline algae[70,71]. The given examples

highlight that the establishment and survivability of coastal (kelp forest) communities are closely tied to the composition of the coralline algal community. Changes in the community caused by reduced light are thus likely to have strong impacts on ecosystem structure and functioning. However, our results also show that similar impacts can be expected if light intensity increases, for example due to the removal of canopy. Indeed, partial or complete canopy removal often results in the replacement of sub-canopy, low-light species (e.g. non-geniculate corallines) with high-light species (e.g. turf algae or geniculate corallines)[72–74] and a reduced coralline diversity[75]. While the removal of the canopy signifies a rather dramatic event (which could conceivably occur in regions with acute and/or prolonged kelp retraction), we show that already relatively small increases and decreases in light intensity are enough to elicit pronounced organismal responses. These are likely to carry over to the community and ecosystem level. Any human modification of coastal light should thus be averted since this likely exacerbates variations in light availability induced by changes in cloud cover[76], storm frequency/intensity[77–79], and sea level[80,81]. Optimal light levels on the other hand could bolster the ecosystem resilience to environmental change.

Conclusion

Results show that light-enhanced calcification of coralline algae is not a result of the removal of CO_2 from CF. Instead, it appears that light-enhanced calcification is the result of an elevated pH_{DBL} which raises pH_{CF} and the increased pumping of ions into and out of the CF. Ion pumping is likely to be stimulated by light and perhaps energetically supported by the increasing photosynthetic output. However, the higher metabolic activity increases the release of respiratory CO_2 at night. This likely decreases pH_{DBL} and increases night-time dissolution that can reduce the positive effect of light on growth. This, together with any change in ion pumping, can create situations in which irradiance, photosynthesis, and growth are no longer positively correlated with each other.

Our results also revealed the existence of two different, morphology-related calcification modes in coralline algae and show that Mg incorporation is likely to be driven primarily by the $[Mg]_{CF}/[Ca]_{CF}$ ratio. However, to validate our observations, we need to directly measure $[Ca]_{CF}$, pH_{CF}, $[DIC]_{CF}$ and pH_{DBL} at the same time, which should be the aim of future research. Future studies should also include species from different habitats and geographic regions since they are likely to respond differently. Our observations should also be corroborated by direct measurements in the field and ecological studies should aim to measure responses of low-light species/communities to changing irradiance. In such communities the impacts of a modified light regime appear to be disproportionate, and changes in performance, productivity, and community composition are likely to precede rather than follow those of (iconic) high-light species. This study increases our knowledge about the calcification physiology of coralline algae and provides mechanistic insights into the role of light in calcification processes. The study demonstrates that the need to preserve pristine coastal light environments is paramount, since suboptimal light conditions are very likely to alter coralline algal physiology, fitness and competitive outcomes that change their communities in unpredictable ways.

Declarations

Acknowledgements

We thank J. Van der Sman for his assistance during collection; J. Delgado and J. Brown for their help with carbon isotope measurements; Y. Tassin for creating a R script for A_T analysis; and R. D'Archino for training in molecular identification. ECK and CEC were supported by a Rutherford Discovery Fellowship from The Royal Society of New Zealand Te Apārangi (no. RDF-VUW1701) awarded to CEC. Part of the research was paid for by a grant awarded to CEC and WAN by the Victoria University of Wellington University Research Fund.

Author contributions

ECK, CEC, WAN, SKD designed the research. ECK wrote the paper. ECK, AC and CEC ran the experiment. ECK and WAN conducted morphological and molecular species identification. ECK performed the statistical analysis. ELR, JG and SJB contributed reagents/materials/analysis tools. All authors edited the manuscript, or provided intellectual input, and agreed to its submission.

Additional Information

Supplementary information accompanies this paper at (to be decided).

Competing Interests The authors declare no competing interests.

References

1. Nelson, W. A. Calcified macroalgae - critical to coastal ecosystems and vulnerable to change: a review. *Mar. Freshw. Res.* **60**, 787 (2009).

2. Kamenos, N. A., Moore, P. G. & Hall-Spencer, J. M. Nursery-area function of maerl grounds for juvenile queen scallops. *Mar. Ecol. Prog. Ser.* **274**, 183–189 (2004).

3. Adey, W. H. Coral reefs: Algal structured and mediated ecosystems in shallow, turbulent, alkaline waters. *J. Phycol.* **34**, 393–406 (1998).

4. Kamenos, N. A., Moore, P. G. & Hall-Spencer, J. M. Small-scale distribution of juvenile gadoids in shallow inshore waters; what role does maerl play? *ICES J. Mar. Sci.* **61**, 422–429 (2004).

5. Bosence, D. W. J. Coralline algal reef frameworks. *J. Geol. Soc. London.* **140**, 365–376 (1983).

6. Nelson, W., D'Archino, R., Neill, K. & Farr, T. Macroalgal diversity associated with rhodolith beds in Northern New Zealand. *Cryptogam. Algol.* **35**, 27–47 (2014).

7. Kitamura, H., Kitahara, S. & Koh, H. B. The induction of larval settlement and metamorphosis of two sea urchins, *Pseudocentrotus depressus* and *Anthocidaris crassispina*, by free fatty acids extracted from the coralline red alga *Corallina pilulifera*. *Mar. Biol.* **115**, 387–392 (1993).

8. Pearce, C. M. & Scheibling, R. E. Effect of macroalgae, microbial films, and conspecifics on the induction of metamorphosis of the green sea urchin *Strongylocentrotus droebachiensis* (Müller). *J. Exp. Mar. Bio. Ecol.* **147**, 147–162 (1991).

9. Morse, D. E. Flypapers for Coral and Other Planktonic Larvae. *Bioscience* **46**, 254–262 (1996).

10. Roberts, R. D., Kaspar, H. F. & Barker, R. J. Settlement of abalone (*Haliotis iris*) larvae in response to five species of coralline algae. *J. Shellfish Res.* **23**, 975–987 (2004).

11. Van Der Heijden, L. H. & Kamenos, N. A. Reviews and syntheses: Calculating the global contribution of coralline algae to total carbon burial. *Biogeosciences* **12**, 6429–6441 (2015).

12. Bensoussan, N. & Gattuso, J. P. Community primary production and calcification in a NW Mediterranean ecosystem dominated by calcareous macroalgae. *Mar. Ecol. Prog. Ser.* **334**, 37–45 (2007).

13. Chisholm, J. R. M. Primary productivity of reef-building crustose coralline algae. *Limnol. Oceanogr.* **48**, 1376–1387 (2003).

14. Kroeker, K. J. *et al.* Impacts of ocean acidification on marine organisms: quantifying sensitivities and interaction with warming. *Glob. Chang. Biol.* **19**, 1884–96 (2013).

15. Ordoñez, A., Kennedy, E. V. & Diaz-Pulido, G. Reduced spore germination explains sensitivity of reef-building algae to climate change stressors. *PLoS One* **12**, e0189122 (2017).

16. Guenther, R., Miklasz, K., Carrington, E. & Martone, P. T. Macroalgal spore dysfunction: ocean acidification delays and weakens adhesion. *J. Phycol.* **54**, 153–158 (2018).

17. Comeau, S., Edmunds, P. J., Spindel, N. B. & Carpenter, R. C. The responses of eight coral reef calcifiers to increasing partial pressure of CO_2 do not exhibit a tipping point. *Limnol. Oceanogr.* **58**, 388–398 (2013).

18. Cornwall, C. E., Comeau, S. & McCulloch, M. T. Coralline algae elevate pH at the site of calcification under ocean acidification. *Glob. Chang. Biol.* **23**, 4245–4256 (2017).

19. Comeau, S., Cornwall, C. E., DeCarlo, T. M., Krieger, E. & McCulloch, M. T. Similar controls on calcification under ocean acidification across unrelated coral reef taxa. *Glob. Chang. Biol.* **24**, 4857–4868 (2018).

20. Cornwall, C. E. *et al.* Resistance of corals and coralline algae to ocean acidification: physiological control of calcification under natural pH variability. *Proc. R. Soc. B Biol. Sci.* **285**, 20181168 (2018).

21. Kirk, J. T. O. Effects of suspensoids (turbidity) on penetration of solar radiation in aquatic ecosystems. *Hydrobiologia* **125**, 195–208 (1985).

22. Benedetti-Cecchi, L. *et al.* Predicting the consequences of anthropogenic disturbance: large-scale effects of loss of canopy algae on rocky shores. *Mar. Ecol. Prog. Ser.* **214**, 137–150 (2001).

23. Gorgula, S. & Connell, S. Expansive covers of turf-forming algae on human-dominated coast: the relative effects of increasing nutrient and sediment loads. *Mar. Biol.* **145**, 613–619 (2004).

24. Airoldi, L. The effects of sedimentation on rocky costal assemblages. *Oceanogr. Mar. Biol. Annu. Rev.* **41**, 161–236 (2003).

25. Hepburn, C. D. *et al.* Diversity of carbon use strategies in a kelp forest community: implications for a high CO_2 ocean. *Glob. Chang. Biol.* **17**, 2488–2497 (2011).

26. Suggett, D. J. *et al.* Light availability determines susceptibility of reef building corals to ocean acidification. *Coral Reefs* **32**, 327–337 (2013).

27. Beck, M. & Airoldi, L. Loss, Status and Trends for Coastal Marine Habitats of Europe. *Oceanogr. Mar. Biol. an Annu. Rev.* **45**, 345–405 (2007).

28. McGranahan, G., Balk, D. & Anderson, B. The rising tide: Assessing the risks of climate change and human settlements in low elevation coastal zones. *Environ. Urban.* **19**, 17–37 (2007).

29. Goreau, T. F. Calcium carbonate deposition by coralline algae and corals in relation to their roles as reef builders. *Ann. N. Y. Acad. Sci.* **109**, 127–167 (1963).

30. Borowitzka, M. A. & Larkum, A. W. D. Calcification in algae: Mechanisms and the role of metabolism. *CRC. Crit. Rev. Plant Sci.* **6**, 1–45 (1987).

31. Borowitzka, M. A. Photosynthesis and calcification in the articulated coralline red algae *Amphiroa anceps* and *A. foliacea*. *Mar. Biol.* **62**, 17–23 (1981).

32. Hurd, C. L. *et al.* Metabolically induced pH fluctuations by some coastal calcifiers exceed projected 22nd century ocean acidification: A mechanism for differential susceptibility? *Glob. Chang. Biol.* **17**, 3254–3262 (2011).

33. Cornwall, C. E., Hepburn, C. D., Pilditch, C. A. & Hurd, C. L. Concentration boundary layers around complex assemblages of macroalgae: Implications for the effects of ocean acidification on understory coralline algae. *Limnol. Oceanogr.* **58**, 121–130 (2013).

34. Cornwall, C. E. *et al.* Diffusion Boundary Layers Ameliorate the Negative Effects of Ocean Acidification on the Temperate Coralline Macroalga *Arthrocardia corymbosa*. *PLoS One* **9**, e97235 (2014).

35. Comeau, S. *et al.* Flow-driven micro-scale pH variability affects the physiology of corals and coralline algae under ocean acidification. *Sci. Rep.* **9**, 1–12 (2019).

36. Comeau, S. *et al.* Resistance to ocean acidification in coral reef taxa is not gained by acclimatization. *Nat. Clim. Chang.* **9**, 477–483 (2019).

37. Kottmeier, D. M., Rokitta, S. D. & Rost, B. H^+-driven increase in CO_2 uptake and decrease in HCO_3^- uptake explain coccolithophores' acclimation responses to ocean acidification. *Limnol. Oceanogr.* **61**, 2045–2057 (2016).

38. Liu, Y. W., Eagle, R. A., Aciego, S. M., Gilmore, R. E. & Ries, J. B. A coastal coccolithophore maintains pH homeostasis and switches carbon sources in response to ocean acidification. *Nat. Commun.* **9**, 1–12 (2018).

39. Allemand, D. *et al.* Biomineralisation in reef-building corals: From molecular mechanisms to environmental control. *Comptes Rendus - Palevol* **3**, 453–467 (2004).

40. Chalker, B. E. & Taylor, D. L. Light-Enhanced Calcification, and the Role of Oxidative Phosphorylation in Calcification of the Coral *Acropora cervicornis*. *Proc. R. Soc. B Biol. Sci.* **190**, 323–331 (1975).

41. Holcomb, M., Tambutté, E., Allemand, D. & Tambutté, S. Light enhanced calcification in *Stylophora pistillata*: Effects of glucose, glycerol and oxygen. *PeerJ* **2014**, 1–18 (2014).

42. Farr, T., Broom, J., Hart, D., Neill, K. & Nelson, W. (2009) Common coralline algae of northern New Zealand: An identification guide. *NIWA Information Series No. 70.*

43. Twist, B. A. *et al.* High diversity of coralline algae in New Zealand revealed: Knowledge gaps and implications for future research. *PLoS One* **14**, 1–21 (2019).

44. Yoon, H. S., Hackett, J. D. & Bhattacharya, D. A single origin of the peridinin- and fucoxanthin-containing plastids in dinoflagellates through tertiary endosymbiosis. *Proc. Natl. Acad. Sci.* **99**, 11724–11729 (2002).

45. Twist, B. A. *et al.* The need to employ reliable and reproducible species identifications in coralline algal research. *Mar. Ecol. Prog. Ser.* **654**, 225–231 (2020).

46. Tait, L. W., Hawes, I. & Schiel, D. R. Shining Light on Benthic Macroalgae: Mechanisms of Complementarity in Layered Macroalgal Assemblages. *PLoS One* **9**, e114146 (2014).

47. Dickson, A. G., Sabine, C. L. and Christian, J. R. (Eds.) 2007. Guide to best practices for ocean CO_2 measurements. PICES Special Publication 3, pp 191.

48. R Core Team (2021). R: A language and environment for statistical computing. R Foundation for Statistical Computing, Vienna, Austria. URL: https://www.R-project.org/.

49. Jokiel, P., Maragos, J. & Franzisket, L. Coral growth: buoyant weight technique. *Coral reefs Res. methods* 529–541 (1978).

50. DeCarlo, T. M. *et al.* Coral calcifying fluid aragonite saturation states derived from Raman spectroscopy. *Biogeosciences* **14**, 5253–5269 (2017).

51. Urmos, J., Sharma, S. K. & Mackenzie, F. T. Characterization of some biogenic carbonates with Raman spectroscopy. *Am. Mineral.* **76**, 641–646 (1991).

52. Perrin, J. *et al.* Raman characterization of synthetic magnesian calcites. *Am. Mineral.* **101**, 2525–2538 (2016).

53. Paul, D., Skrzypek, G. & Fórizs, I. Normalization of measured stable isotopic compositions to isotope reference scales - A review. *Rapid Commun. Mass Spectrom.* **21**, 3006–3014 (2007).

54. Walsby, A. E. Numerical integration of phytoplankton photosynthesis through time and depth in a water column. *New Phytol.* **136**, 189–209 (1997).

55. Sampath-Wiley, P. & Neefus, C. D. An improved method for estimating R-phycoerythrin and R-phycocyanin contents from crude aqueous extracts of *Porphyra* (Bangiales, Rhodophyta). *J. Appl. Phycol.* **19**, 123–129 (2007).

56. Ritchie, R. J. Universal chlorophyll equations for estimating chlorophylls *a*, *b*, *c*, and *d* and total chlorophylls in natural assemblages of photosynthetic organisms using acetone, methanol, or ethanol solvents. *Photosynthetica* **46**, 115–126 (2008).

57. Marsh, J. A. Primary productivity of reef-building calcareous red algae. *Ecology* **51.2**, 255–265 (1970).

58. Pentecost, A. Calcification and photosynthesis in *Corallina officinalis* L. Using the $^{14}CO_2$ method. *Br. Phycol. J.* **13**, 383–390 (1978).

59. Comeau, S., Carpenter, R. C. & Edmunds, P. J. Effects of irradiance on the response of the coral *Acropora pulchra* and the calcifying alga *Hydrolithon reinboldii* to temperature elevation and ocean acidification. *J. Exp. Mar. Bio. Ecol.* **453**, 28–35 (2014).

60. Martin, S., Cohu, S., Vignot, C., Zimmerman, G. & Gattuso, J. P. One-year experiment on the physiological response of the Mediterranean crustose coralline alga, *Lithophyllum cabiochae*, to elevated pCO_2 and temperature. *Ecol. Evol.* **3**, 676–693 (2013).

61. Egilsdottir, H., Olafsson, J. & Martin, S. Photosynthesis and calcification in the articulated coralline alga *Ellisolandia elongata* (Corallinales, Rhodophyta) from intertidal rock pools. *Eur. J. Phycol.* **51**, 59–70 (2016).

62. Chisholm, J. R. M. Calcification by Crustose Coralline Algae on the Northern Great Barrier Reef, Australia. *Limnol. Oceanogr.* **45**, 1476–1484 (2000).

63. Martin, S., Castets, M. D. & Clavier, J. Primary production, respiration and calcification of the temperate free-living coralline alga *Lithothamnion corallioides*. *Aquat. Bot.* **85**, 121–128 (2006).

64. Ries, J. B. Mg fractionation in crustose coralline algae: Geochemical, biological, and sedimentological implications of secular variation in the Mg/Ca ratio of seawater. *Geochim. Cosmochim. Acta* **70**, 891–900 (2006).

65. Ross, C. L., Schoepf, V., DeCarlo, T. M. & McCulloch, M. T. Mechanisms and seasonal drivers of calcification in the temperate coral *Turbinaria reniformis* at its latitudinal limits. *Proc. R. Soc. B Biol. Sci.* **285**, 20180215 (2018).

66. Cornwall, C. E. *et al.* A coralline alga gains tolerance to ocean acidification over multiple generations of exposure. *Nat. Clim. Chang.* **10**, 143–146 (2020).

67. Morse, J. W., Andersson, A. J. & Mackenzie, F. T. Initial responses of carbonate-rich shelf sediments to rising atmospheric pCO_2 and 'ocean acidification': Role of high Mg-calcites. *Geochim. Cosmochim. Acta* **70**, 5814–5830 (2006).

68. Moberly, R. Composition of magnesian calcites of algae and pelecypods by electron microprobe analysis. *Sedimentology* **11**, 61–82 (1968).

69. Barner, A. K., Hacker, S. D., Menge, B. A. & Nielsen, K. J. The complex net effect of reciprocal interactions and recruitment facilitation maintains an intertidal kelp community. *J. Ecol.* **104**, 33–43 (2016).

70. Parada, G. M., Martínez, E. A., Aguilera, M. A., Oróstica, M. H. & Broitman, B. R. Interactions between kelp spores and encrusting and articulated corallines: recruitment challenges for Lessonia spicata. **60**, 619–625 (2017).

71. Kim, M. *et al.* Multiple allelopathic activity of the crustose coralline alga *Lithophyllum yessoense* against settlement and germination of seaweed spores. *J. Appl. Phycol.* **16**, 175–179 (2004).

72. Irving, A. D., Connell, S. D. & Elsdon, T. S. Effects of kelp canopies on bleaching and photosynthetic activity of encrusting coralline algae. *J. Exp. Mar. Bio. Ecol.* **310**, 1–12 (2004).

73. Connell, S. D. The monopolization of understorey habitat by subtidal encrusting coralline algae: A test of the combined effects of canopy-mediated light and sedimentation. *Mar. Biol.* **142**, 1065–1071 (2003).

74. Wernberg, T., Couraudon-réale, M., Tuya, F. & Thomsen, M. Disturbance intensity, disturbance extent and ocean climate modulate kelp forest understory communities. *Mar. Ecol. Prog. Ser.* **651**, 57–69 (2020).

75. Hind, K. R. *et al.* Trophic control of cryptic coralline algal diversity. *Proc. Natl. Acad. Sci. U. S. A.* **116**, 15080–15085 (2019).

76. Anthony, K. R. N., Ridd, P. V., Orpin, A. R., Larcombe, P. & Lough, J. Temporal variation of light availability in coastal benthic habitats: Effects of clouds, turbidity, and tides. *Limnol. Oceanogr.* **49**, 2201–2211 (2004).

77. Byrnes, J. E. *et al.* Climate-driven increases in storm frequency simplify kelp forest food webs. *Glob. Chang. Biol.* **17**, 2513–2524 (2011).

78. Munks, L. S., Harvey, E. S. & Saunders, B. J. Storm-induced changes in environmental conditions are correlated with shifts in temperate reef fish abundance and diversity. *J. Exp. Mar. Bio. Ecol.* **472**, 77–88 (2015).

79. Fettweis, M. *et al.* Storm influence on SPM concentrations in a coastal turbidity maximum area with high anthropogenic impact (southern North Sea). *Cont. Shelf Res.* **30**, 1417–1427 (2010).

80. Saunders, M. I. *et al.* Coastal retreat and improved water quality mitigate losses of seagrass from sea level rise. *Glob. Chang. Biol.* **19**, 2569–2583 (2013).

81. Davis, T. R., Harasti, D., Smith, S. D. A. & Kelaher, B. P. Using modelling to predict impacts of sea level rise and increased turbidity on seagrass distributions in estuarine embayments. *Estuar. Coast. Shelf Sci.* **181**, 294–301 (2016).

Figures

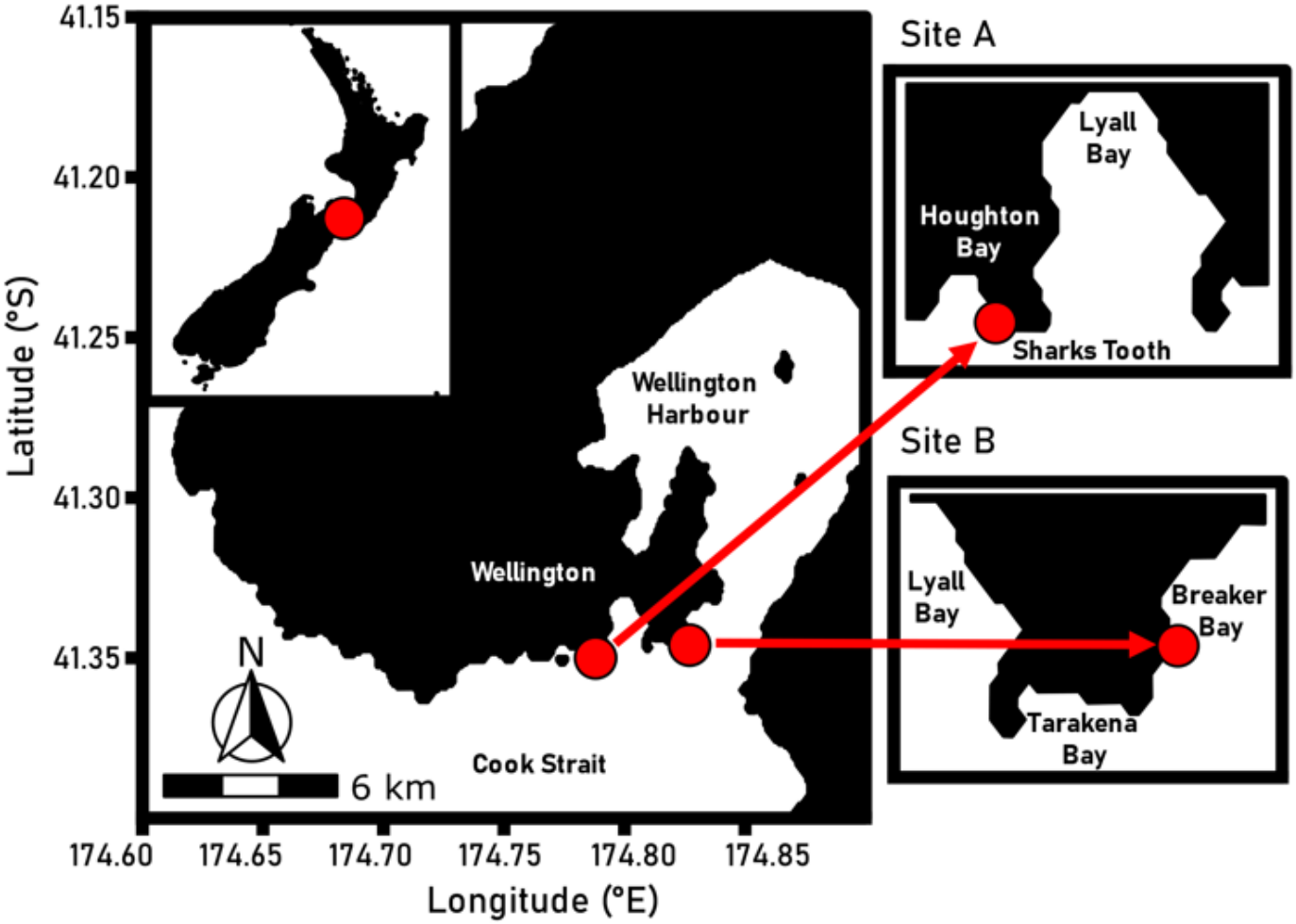

Figure 1

Map showing the location of sampling sites A/Sharks Tooth and B/Breaker Bay, both located in Te Moana-o-Raukawa Cook Strait, Te Whanganui a Tara Wellington, at the southern end of Aotearoa New Zealand's North Island.

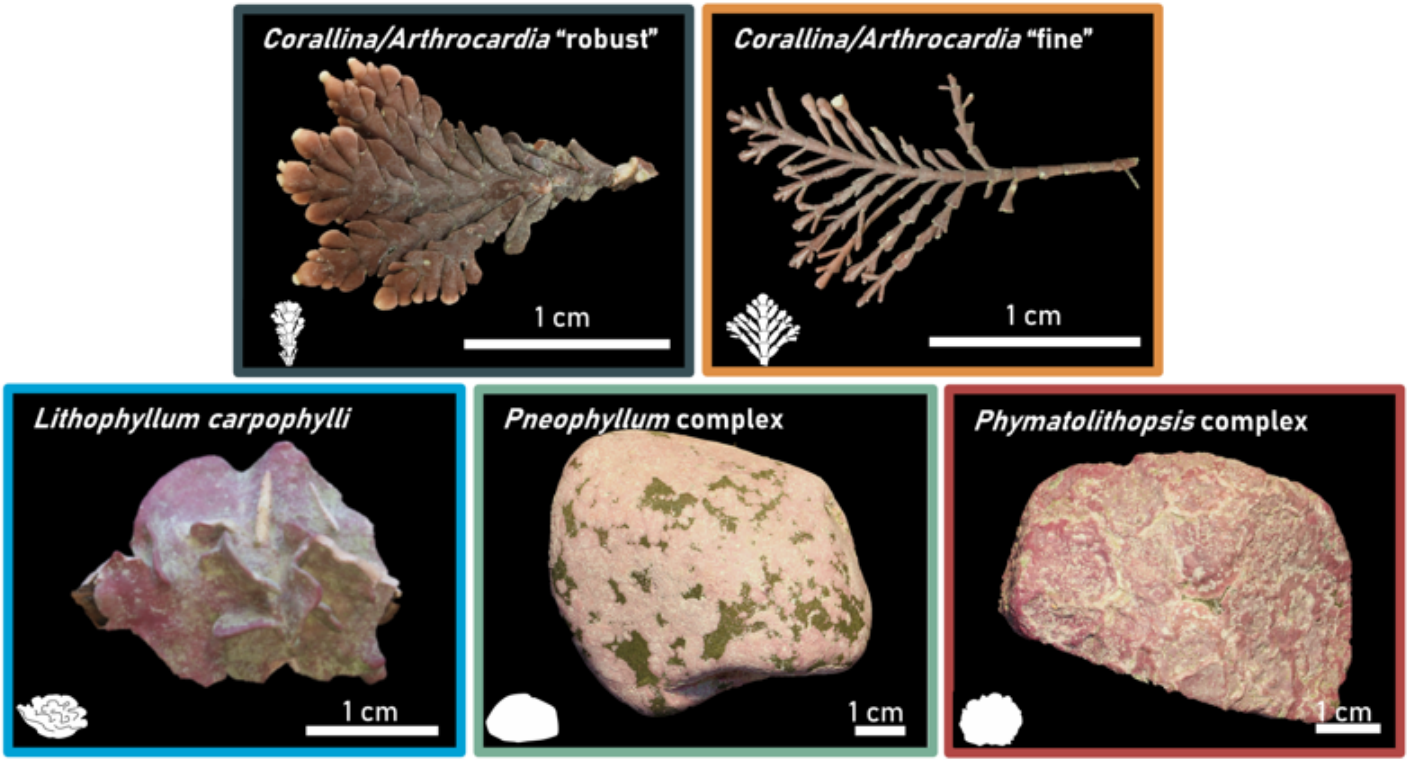

Figure 2

Pictures showing the morphology of the five study species/species complexes. Colours and schematics associated with each morphology will be used in various figures throughout the remainder of the text.

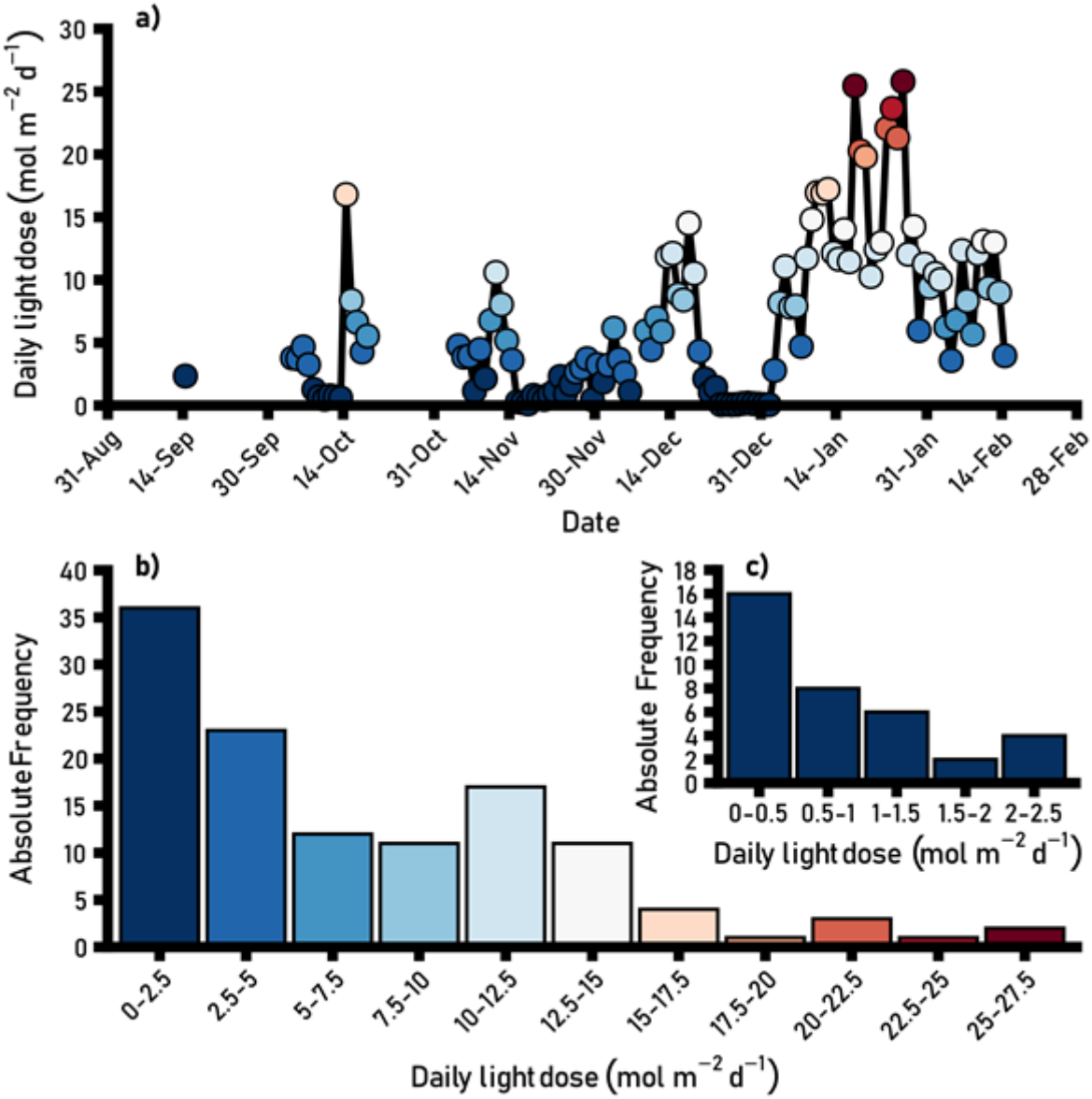

Figure 3

a) Daily light dose (mol photons m^{-2} d^{-1}) below the kelp canopy at field site A/Sharks Tooth measured over the 2020/21 New Zealand summer (mid-September 2020 – mid-February 2021; n=117). b) Absolute frequency of daily light doses measured over this period grouped in categories. c) Absolute frequency of low light events (daily light doses 0–2.5 mol photons m^{-2} d^{-1}) which were measured on ~30% of all days. The light levels chosen for this experiment would fall into the categories 0.5–1, 1–1.5, 1.5–2 and 2–2.5, respectively. Logging interval of integrating light loggers was set to five minutes.

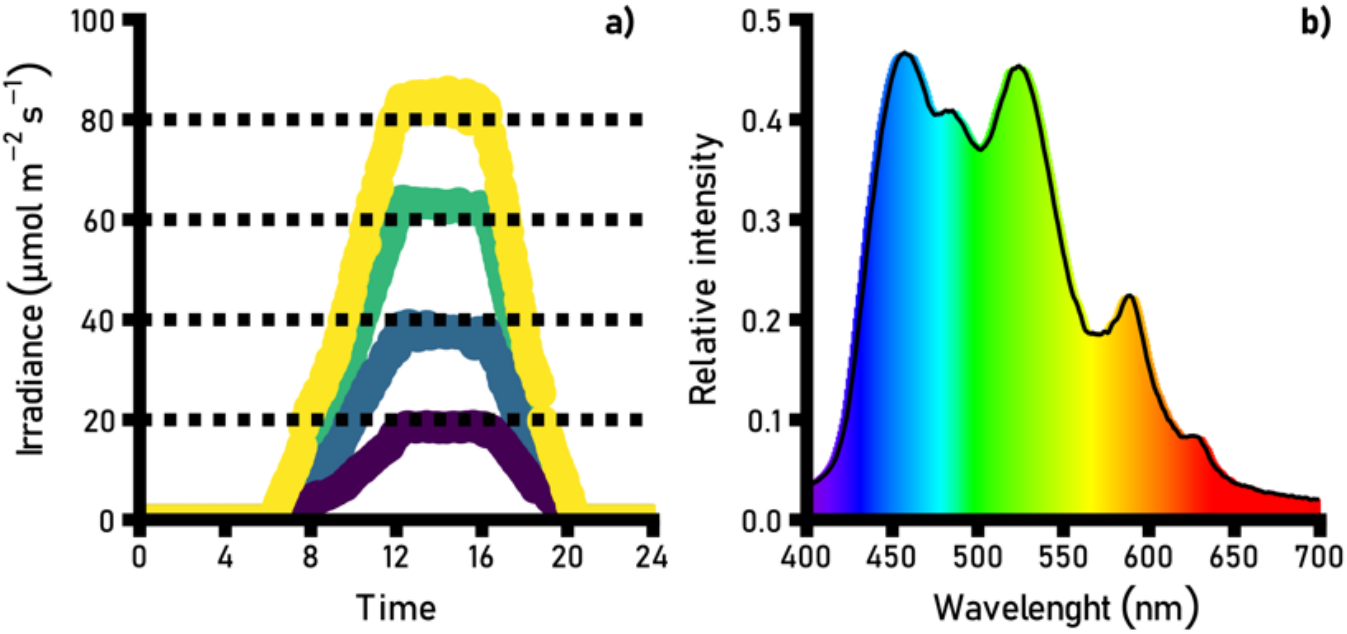

Figure 4

a) Light levels measured during a 24 h cycle in four of the experimental tanks (colours indicate light treatments). b) Light spectrum of light emitting diode (LED) panels used in the experiment.

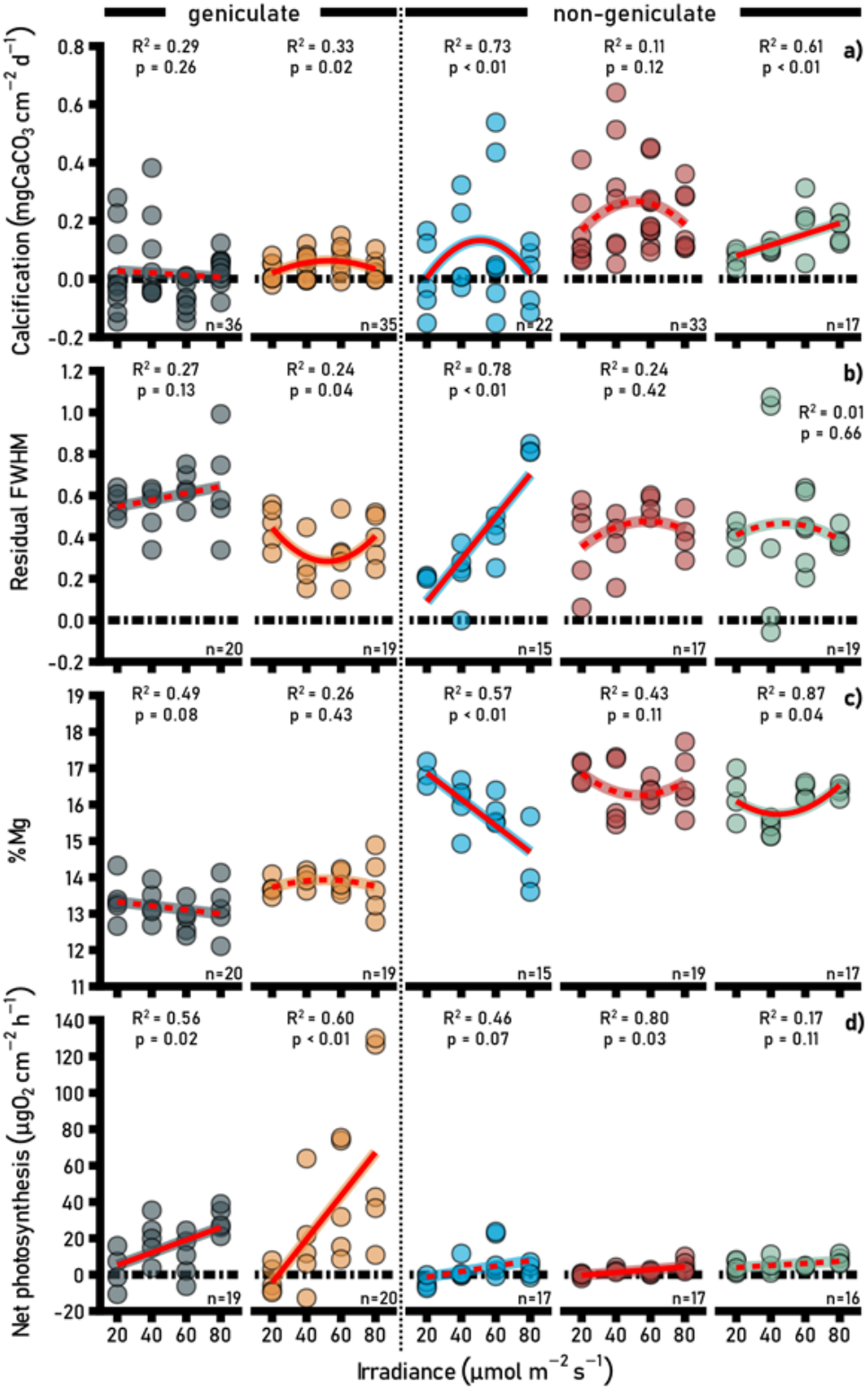

Figure 5

Effect of irradiance on: a) mean net calcification, b) residual FWHM, c) magnesium (Mg) content and, d) net photosynthesis of study species. Points show individual values and colours indicate species (grey = *Corallina*/ *Arthrocardia* "robust"; yellow = *Corallina*/ *Arthrocardia* "fine"; blue = *L. carpophylli*; red = *Phymatolithopsis* complex; green = *Pneophyllum* complex). Lines indicate whether parabolic or linear models were fitted to the data (dashed = non-significant; solid = significant). Proportions of variation (R^2)

and probability values (p-values) were obtained from full linear mixed effect models, and n = number of replicates.

Supplementary Files

This is a list of supplementary files associated with this preprint. Click to download.

- Supplementarymaterial.docx